PAPER

Pulling adsorbed self-avoiding walks from a surface

IOP Publishing Journal of Physics A: Mathematical and Theoretical
J. Phys. A: Math. Theor. **47** (2014) 015004 (15pp) doi:10.1088/1751-8113/47/1/015004

Pulling adsorbed self-avoiding walks from a surface

Anthony J Guttmann[1], **I Jensen**[1] **and S G Whittington**[2]

[1] ARC Centre of Excellence for Mathematics and Statistics of Complex Systems, Department of Mathematics and Statistics, The University of Melbourne, Victoria 3010, Australia
[2] Department of Chemistry, University of Toronto, Toronto, Canada

E-mail: tonyg@ms.unimelb.edu.au, iwan@ms.unimelb.edu.au and swhittin@chem.utoronto.ca

Received 27 September 2013, revised 7 November 2013
Accepted for publication 15 November 2013
Published 11 December 2013

Abstract

We consider a self-avoiding walk model of polymer adsorption where the adsorbed polymer can be desorbed by the application of a force, concentrating on the case of the square lattice. Using series analysis methods we investigate the behaviour of the free energy of the system when there is an attractive potential ϵ with the surface and a force f applied at the last vertex, normal to the surface, and extract the phase boundary between the ballistic and adsorbed phases. We believe this to be exact to graphical accuracy. We give precise estimates of the location of the transition from the free phase to the ballistic phase, which we find to be at $y_c = \exp(f/k_BT_c) = 1$, and from the free phase to the adsorbed phase, which we estimate to be at $a_c = \exp(-\epsilon/k_BT_c) = 1.775\,615 \pm 0.000\,005$. In addition we prove that the phase transition from the ballistic to the adsorbed phase is first order.

PACS numbers: 05.50.+q, 64.60.De, 68.47.Pe, 82.35.Gh

(Some figures may appear in colour only in the online journal)

1. Introduction

The theory of polymer adsorption [7, 21] has a long history [33, 35]. For linear polymers a variety of models have been considered including random walks [13, 33, 37], directed and partially directed walks [10, 22, 39] and self-avoiding walks (SAW) [2, 3, 11, 15, 17, 20, 24]. In this paper we shall be concerned with the SAW model for which there are a few rigorous results [15, 20] as well as extensive numerical investigations (see for instance [3, 11, 17, 24]).

The invention of micro-manipulation techniques such as atomic force microscopy [40] which allow adsorbed polymer molecules to be pulled off a surface [16] has led to the

development of theories of adsorbed polymers subject to a force [29, 31, 32, 36, 37]. Much of this work has focused on random, directed and partially directed walk models but there has been some numerical work on the SAW model [18, 29, 30] and a recent rigorous treatment [25] which establishes the existence of a phase boundary between an adsorbed phase and a ballistic phase when the force is applied normal to the surface. In this paper we use exact enumeration and series analysis techniques to identify this phase boundary for SAW on the square lattice. We also make precise estimates of the critical points for adsorption with no force and for the transition to the ballistic phase with no surface interaction, and various relevant critical exponents. For a brief discussion of critical exponents appearing in this problem see [2] or [11].

2. Definitions and review of rigorous results

Consider the square lattice $\mathbb{Z}^2$ where the vertices have integer coordinates. We write (x_i, y_i), $i = 0, 1, 2, \ldots n$ for the coordinates of the ith vertex of an n-step SAW on $\mathbb{Z}^2$. The number of n-step SAW from the origin is denoted by c_n. It is known that $\lim_{n\to\infty} n^{-1} \log c_n = \log \mu$ exists [14], where μ is the *growth constant* of SAW on this lattice.

A *positive walk* is a SAW on $\mathbb{Z}^2$ that starts at the origin and is constrained to have $y_i \geqslant 0$ for all $0 \leqslant i \leqslant n$. The number of n-step positive walks from the origin is denoted by c_n^+. It is known that $\lim_{n\to\infty} n^{-1} \log c_n^+ = \log \mu$ [38]. Vertices of a positive walk with $y_i = 0$ are *visits* to the surface although, by convention, the vertex at the origin is not counted as a visit. We say that the walk has *height* h if for the last vertex $y_n = h$. The number of positive walks of n-steps from the origin, with v visits and height h is denoted by $c_n^+(v, h)$. The corresponding partition function is

$$C_n(a, y) = \sum_{v,h} c_n^+(v, h) a^v y^h. \tag{1}$$

If ϵ is the energy associated with a visit and f is the force applied at the last vertex, normal to the surface,

$$a = \exp[-\epsilon/k_B T] \quad \text{and} \quad y = \exp[f/k_B T] \tag{2}$$

where k_B is Boltzmann's constant and T is the absolute temperature. If no force is applied $y = 1$ and the appropriate partition function is $C_n(a, 1)$ while if there is no interaction with the surface $a = 1$ and the appropriate partition function is $C_n(1, y)$.

It is known [15] that the limit

$$\lim_{n\to\infty} n^{-1} \log C_n(a, 1) \equiv \kappa(a) \tag{3}$$

exists and that $\kappa(a)$ is a convex function of $\log a$. There exists a value of $a = a_c^o > 1$ such that $\kappa(a) = \log \mu$ for $a \leqslant a_c^o$ and $\kappa(a)$ is strictly monotone increasing for $a > a_c^o$. Therefore the free energy $\kappa(a)$ is non-analytic at $a = a_c^o$ [15] and this corresponds to the adsorption transition in the absence of a force. For $a > a_c^o$, in the adsorbed phase,

$$\lim_{n\to\infty} \frac{\langle v \rangle}{n} > 0 \tag{4}$$

while, for $a < a_c^o$, $\langle v \rangle = o(n)$. Here $\langle \cdots \rangle$ denotes expectation.

Similarly it is known [23] that the limit

$$\lim_{n\to\infty} n^{-1} \log C_n(1, y) \equiv \lambda(y) \tag{5}$$

exists and $\lambda(y)$ is a convex function of $\log y$. There is a critical point $y_c^o \geqslant 1$ such that $\lambda(y) = \log \mu$ for $y \leqslant y_c^o$ and $\lambda(y)$ is strictly monotone increasing for $y > y_c^o$ [23]. The critical point corresponds to a transition from a free phase where $\langle h \rangle = o(n)$ to a ballistic phase where

$$\lim_{n\to\infty} \frac{\langle h \rangle}{n} > 0. \tag{6}$$

There are good reasons to believe [19, 23] that $y_c^o = 1$.

For the full two variable model it has recently been shown [25] that the limiting free energy

$$\psi(a, y) = \lim_{n\to\infty} n^{-1} \log C_n(a, y) \tag{7}$$

exists. $\psi(a, y)$ is a convex function of $\log a$ and $\log y$ (*i.e.* convex as a surface) and

$$\psi(a, y) = \max[\kappa(a), \lambda(y)]. \tag{8}$$

This implies that there is a *free phase* when $a < a_c^o$ and $y < y_c^o$ where $\langle v \rangle = o(n)$ and $\langle h \rangle = o(n)$ and a strictly monotone curve $y = y_c(a)$ through the point (a_c^o, y_c^o) separating two phases:

(1) an *adsorbed phase* when $a > a_c^o$ and $y < y_c(a)$, and
(2) a *ballistic phase* when $y > \max[y_c^o, y_c(a)]$.

Moreover, for the square lattice, $y_c(a)$ is asymptotic to $y = a$ as $a \to \infty$.

3. Exact enumerations

The algorithm we use to enumerate SAW on the square lattice builds on the pioneering work of Enting [9] who enumerated square lattice self-avoiding polygons (SAP) using the finite lattice method. More specifically our algorithm is based in large part on the one devised by Conway, Enting and Guttmann [6] for the enumeration of SAWs. Many details of our algorithm can be found in [26]. All of the above transfer matrix (TM) algorithms are based on keeping track of the way partially constructed SAW are connected to the left of a cut-line bisecting the given finite lattice (rectangles in the case of the square lattice). Recently Clisby and Jensen [5] devised a new and more efficient implementation of the TM algorithm for SAP. In that implementation we took a new approach and instead kept track of how a partially constructed SAP must connect up to the right of the cut-line. Jensen extended this approach to the enumeration of SAW [27]. Here we briefly describe how this algorithm can be amended to enumerate SAW configurations for the problem we study in this paper.

The first terms in the series for the SAW generating function can be calculated using TM techniques to count the number of walks in rectangles W unit cells wide and L cells long. Any walk spanning such a rectangle has a length of at least $W + L$ steps. By adding the contributions from all rectangles of width $W \leqslant W_{\max}$ (where the choice of $W_{\max}$ depends on available computational resources) and length $W \leqslant L \leqslant 2W_{\max} - W + 1$ the number of walks per vertex of an infinite lattice is obtained correctly up to length $N = 2W_{\max} + 1$.

The basic idea of the algorithm can best be illustrated by considering the specific example of a SAW given in figure 1. Clearly any SAW is topologically equivalent to a line and therefore has exactly two end-points. If we cut the SAW by a vertical line as shown in figure 2 (the dashed line) we see that the SAW is broken into several pieces to the left and right of the cut-line. On *either* side of the cut-line we have a set of arcs connecting two edges on the cut-line and at most two line pieces connected to the end-points of the SAW. As we move the cut-line from left to right we prescribe what must happen in the future, that is how edges are to be connected to the right of the cut-line so as to form a valid SAW. Each end of an arc is assigned one of two

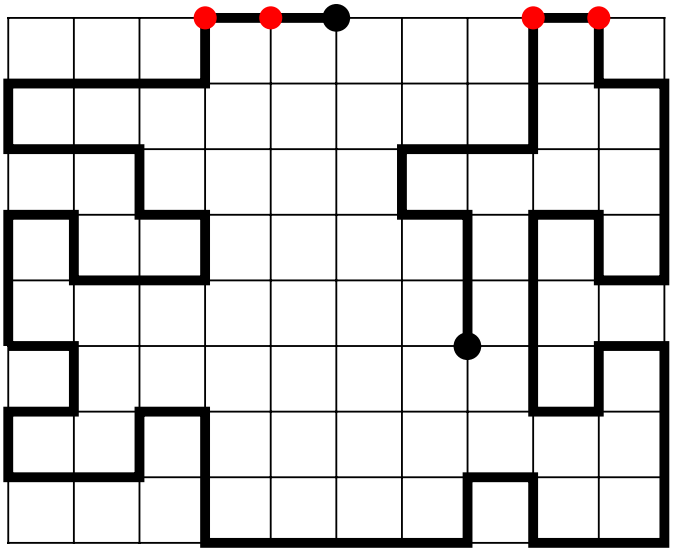

Figure 1. An example of a self-avoiding walk on a 10×8 rectangle. The walk is tethered to the surface, has the end-point at $h = 5$ and four vertices (other than the start-point) in the surface.

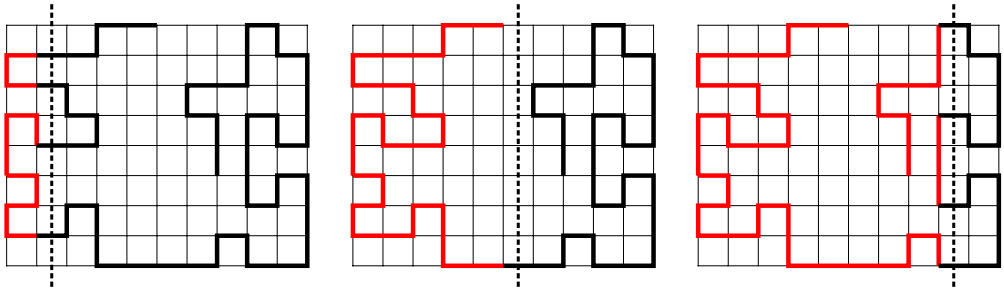

Figure 2. Examples of cut-lines through the SAW of figure 1 such that the signature of the yet to be completed section to the right of the cut-line (black lines) contains, respectively, two, one and no free edges.

labels depending on whether it is the lower or upper end of an arc. Any configuration along the cut-line can thus be represented by a set of edge states $\{\sigma_i\}$, where

$$\sigma_i = \begin{cases} 0 & \text{empty edge,} \\ 1 & \text{lower edge,} \\ 2 & \text{upper edge,} \\ 3 & \text{free edge.} \end{cases} \tag{9}$$

If we read from the bottom to the top, the configuration or signature S along the cut-lines of the SAW in figure 2 are, respectively, $S = \{030\,010\,230\}$, $S = \{300\,000\,000\}$, and $S = \{102\,001\,002\}$. Since crossings are not permitted this encoding uniquely describes how the occupied edges are connected.

The most efficient implementation of the TM algorithm generally involves moving the cut-line in such a way as to build up the lattice vertex by vertex. The sum over all contributing graphs is calculated as the cut-line is moved through the lattice. For each configuration of occupied or empty edges along the intersection we maintain a generating function G_S for partial walks with signature S. In exact enumeration studies such as this G_S is a truncated

polynomial $G_S(x, a)$ where x is conjugate to the number of steps and a to the number of visited vertices in the surface. In a TM update each source signature S (before the boundary is moved) gives rise to a few new target signatures S' (after the move of the boundary line) as $k = 0, 1$ or 2 new edges are inserted with $m = 0$ or 1 surface visits leading to the update $G_{S'}(x, a) = G_{S'}(x, a) + x^k a^m G_S(x, a)$. Once a signature S has been processed it can be discarded.

Some minor changes to the basic algorithm described in [27] are required in order to enumerate the SAW configurations for the problem we study in this paper. Since we are moving the cut-line so as to add one vertex at a time we have complete control over the placement of the end-points of the SAW. In particular, grafting the SAW to the surface can be achieved by forcing the SAW to have a free end (the start-point) on the top of the rectangle. In enumerations of unrestricted SAW one can use symmetry to restrict the TM calculations to rectangles with $W \leqslant N/2 + 1$ and $L \geqslant W$ by counting contributions for rectangles with $L > W$ twice. The grafting of the start-point to the wall breaks the symmetry and we have to consider all rectangles with $W \leqslant N + 1$. The number of signatures one must consider grows exponentially with W. Hence we must minimize the length of the cut-line to obtain an optimal algorithm. To achieve this the TM calculation on the set of rectangles is broken into two sub-sets with $L \geqslant W$ and $L < W$, respectively. The calculations for the sub-set with $L \geqslant W$ is done as outlined above. In the calculations for the sub-set with $L < W$ the boundary line is chosen to be horizontal (rather than vertical) so it cuts across at most $L + 1$ edges. Alternatively, one may view the calculation for the second sub-set as a TM algorithm for SAW with start-point on the left-most border of the rectangle. To keep track of the height h of the end-point we simply specify that it must be placed in a row (or column) h lattice-units from the surface and we then repeat the calculation for all the possible values of h.

We calculated the number of SAW up to length $n = 59$. The calculation was performed in parallel using up to 16 processors, a maximum of some 40 GB of memory and using a total of just under 6000 CPU hours (see [26] for details of the parallel algorithm).

4. Results

In this section we describe the results from series analysis, chiefly using differential approximants [12]. We first discuss the y-dependence of the free energy $\lambda(y)$ when there is no surface interaction, then the a-dependence of the free energy $\kappa(a)$ when there is no applied force and finally the two variable free energy $\psi(a, y)$ when there is both a surface interaction and a force.

4.1. No surface interaction. $a = 1$

If we write

$$H(x, y) = \sum_n C_n(1, y) x^n = \sum_n \mathrm{e}^{\lambda(y)n + o(n)} x^n \tag{10}$$

then $H(x, y)$ will be singular at $x = x_c(y) = \exp[-\lambda(y)]$ and, close to this singularity, $H(x, y)$ is expected to behave as

$$H(x, y) \sim \frac{A}{[x_c(y) - x]^{\gamma(y)}} \tag{11}$$

where $\gamma(y)$ is a critical exponent whose value depends on the value of y.

In table 1 below we give the results of an analysis of the series $H(x, y)$ for various values of y. The resulting estimates of the free energy $\lambda(y) = -\log x_c$ are plotted in figure 3. The

Table 1. SAWs at a surface. Estimates of x_c for $a = 1$ and various y values. For $y > 1$ the singularity is a simple pole. For all y values, there is also an anti-ferromagnetic singularity at $-1/\mu$ with exponent 1.5.

y	x_c	Exponent
0.4	0.379 053	0.186
0.5	0.379 052	0.186
0.6	0.379 052	0.187
0.7	0.379 05	0.195
0.8	0.379 18	0.00
0.9	0.3792	−0.3
0.99	0.379 25	−0.63
0.999	0.379 0837	−0.9328
0.9999	0.379 055	−0.950
0.999 99	0.379 052 628	−0.952 96
0.999 999	0.379 052 29	−0.953 07
1.0	0.379 052 25	−0.953 08
1.000 001	0.379 052 21	−0.953 09
1.000 01	0.379 051 88	−0.953 21
1.0001	0.379 0488	−0.9547
1.001	0.379 019	−0.970
1.01	0.378 62	−1.11
1.02	0.378 04	−1.137
1.04	0.376 49	−1.0
1.06	0.374 63	−0.99
1.08	0.372 65	−0.99
1.1	0.370 564	−1
1.2	0.359 2886	−1
1.3	0.347 5682	−1
1.5	0.324 9328	−1
1.75	0.299 554 7603	−1
2.0	0.277 5487	−1
2.5	0.241 886 2105	−1
3	0.214 449 855	−1
4	0.175 107 0033	−1
5	0.148 208 714 38	−1
7	0.113 657 316 5016	−1
10	0.084 421 281 924	−1
20	0.045 635 244 067	−1
40	0.023 835 934 093 77	−1
60	0.016 137 297 12	−1
90	0.010 872 106 91	−1
150	0.006 579 513 22	−1
250	0.003 968 378 456	−1

series were analysed using second and third order differential approximants [12]. At $y = 1$ the series is well behaved and has critical point $1/\mu$ with exponent $\gamma_1 = 61/64$, the exponent for terminally-attached SAW (TASAW), as one expects [4]. For y just below 1 the series are quite difficult to analyse. Estimates of x_c are close to the known value $1/\mu$. For $y \leqslant 0.7$ this is clearly evident from the analysis. And as y gets smaller still, so that walks ending near to the surface are favoured, it is clear that the exponent is approaching $\gamma_{1,1} = -3/16 = -0.1875$ as expected from the scaling law [1] $2\gamma_1 - \gamma_{11} = \gamma + \nu$. This is the exponent appropriate to arches, often called *loops* in the literature. They are walks in the half-plane whose origin and end-point both lie in the surface. For $y = 0.8$ the series really does suggest that $x_c = 0.379\,18 \pm 0,000\,03$ with an exponent that looks very close to zero. For $y = 0.9$ the approximants suggest that $x_c = 0.3792 \pm 0.0002$, (so could be $1/\mu$) but there is another singularity very close by (at

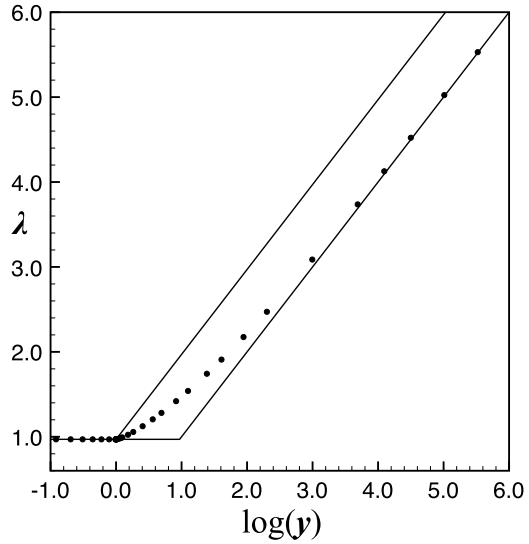

Figure 3. The y-dependence of the free energy $\lambda(y)$. The straight lines indicate the exact lower and upper bounds, where for $\log y < 0$ we know that $\lambda(y) = \log \mu$ while for $\log y > 0$ we know that $\max[\log \mu, \log y] \leqslant \lambda(y) \leqslant \log \mu + \log y$.

around 0.389), and it is known that in such situations the estimate of the location, and exponent, is less trustworthy.

This sort of behaviour is typical of the situation in series analysis when one is in the vicinity of discontinuous change in the critical exponent. The only way a finite series—that is to say, a polynomial approximation to an infinite series—can mimic this discontinuity is by shifting the critical point slightly. So our conclusion is that the observed behaviour is consistent with the known result that $x_c = 1/\mu$ for $y \leqslant 1$, and that the exponent changes discontinuously from $-\gamma_1 = -0.953\,125$ to $-\gamma_{1,1} = 0.1875$ as y decreases below 1.

For $y > 1.04$ the series are beautifully behaved, the singularity is clearly seen to be a simple pole, and we can provide ten digit (or more) accuracy in estimates of the critical point. For $1 < y < 1.04$ we get the sort of behaviour we expect with a discontinuous change in exponent as we transition from an exponent $\gamma_1 \neq 1$ to a simple pole.

So, in summary, it appears that for $y < 1$ we have $x_c = 1/\mu$ and exponent $\gamma_{1,1} = -3/16$; for $y = 1$ we have $x_c = 1/\mu$ and exponent $\gamma_1 = 61/64$ and for $y > 1$ we have x_c monotonically decreasing as y increases, and with a simple pole singularity.

An interesting and unexpected feature is that for all values of y, the location of the *antiferromagnetic* singularity—that is to say, the singularity on the negative real axis, which for unconstrained SAWs is at $x = -1/\mu$, – is unchanged at $-1/\mu$ with exponent $3/2$[3].

A further bonus of this analysis is that the series analysis is exquisitely sensitive to the value of y near $y = 1$. This gives us a method for confirming that $y_c = 1$ [19, 23]. From table 1, giving the results of an analysis of the series $H(x, 1)$ (see the second column of table 2) we find a value of the critical point very close to $1/\mu$. The value of $1/\mu$ is 0.379 052 277 751, with uncertainty in the last digit only [5]. We can vary our estimate of y_c until we get agreement with $1/\mu$, and this turns out to be at $y_c = 0.999\,9995 \pm 0.000\,0005$. We know that $y_c \geqslant 1$,

[3] To be precise, this singularity is less obvious for $y \geqslant 4$. This can be understood from the fact that the radius of convergence of the series decreases as y increases. The location of the anti-ferromagnetic singularity is located at a distance more than twice the radius of convergence when $y \geqslant 4$, so is increasingly difficult to detect. One would have to expect that it is there nonetheless.

Table 2. SAWs at a surface. Estimates of x_c for $y = 1$ and various a values. For $a > a_c$, the singularity is a simple pole. There is also a second, anti-ferromagnetic singularity at $x = x^*$ with exponent $-1/2$.

a	x_c	Exponent	x^*	Exponent
1.3	0.379 052	−0.952	−0.379 05	1.5
1.6	0.379 058	−0.96	−0.3793	1
1.75	0.379 10	−1.31	−0.379 18	0.333
1.775 59	0.379 052 37	−1.4538	−0.379 050	0.256
1.775 615	0.379 052 27	−1.4539	−0.379 050	0.256
1.775 64	0.379 052 17	−1.4541	−0.379 05	0.256
1.775 665	0.379 052 07	−1.4542	−0.379 05	0.256
1.775 69	0.379 051 97	−1.4538	−0.379 05	0.256
1.8	0.378 93	−1.58	−0.378 885	0.189
2.0	0.371 12	−1.06	−0.377	−0.71
2.5	0.332 682	−1.0008	−0.365 065	−0.517
2.75	0.312 5387	−0.999 995	−0.358 06	−0.5002
3.0	0.293 630 848	−1	−0.351 06	−0.5005
4.0	0.232 915 216 0359	−1	−0.325 298	−0.499
5.0	0.191 211 527 263 626	−1	−0.304 03	−0.5005
6.0	0.161 589 812 675 78	−1	−0.286 52	−0.4995
7.5	0.130 751 327 296 498	−1	−0.26538	−0.4994
10.0	0.098 924 010 459 3583	−1	−0.239 12	−0.4996
15.0	0.066 353 637 160 8435	−1	−0.204 74	−0.496
20.0	0.049 869 446 447 162	−1	−0.182 49	−0.503
40	0.024 984 005 079 4006	−1	−0.1367	−0.6
60	0.016 661 962 55	−1	–	–
90	0.011 109 724 48	−1	–	–
150	0.006 666 368 4218	−1	–	–
250	0.003 999 935 75	−1	–	–

so combining our numerical results with this rigorous result, we conclude that $y_c = 1$. So it seems that for $y = y_c$ the exponent is given by γ_1, and that this changes discontinuously to a simple pole for $y > y_c$. For $y < y_c$ the evidence strongly suggests that the exponent is given by $\gamma_{1,1}$.

4.2. No applied force. $y = 1$

Define the generating function

$$K(x, a) = \sum_n C_n(a, 1)x^n = \sum_n e^{\kappa(a)n+o(n)}x^n. \tag{12}$$

$K(x, a)$ will be singular at $x = x_c(a) = \exp[-\kappa(a)]$ and, close to this singularity, $K(x, a)$ should behave as

$$K(x, a) \sim \frac{B}{[x_c(a) - x]^{\gamma(a)}} \tag{13}$$

where $\gamma(a)$ is a critical exponent whose value depends on the value of a.

We have analysed the series $K(x, a)$, corresponding to the 'no force' situation. As in the previous 'no interactions' case, we find that the series is exquisitely sensitive to the value of a_c. The best estimate [3] currently is $a_c = 1.775\,64$, with errors expected to be confined to the last quoted digit. That estimate is a comparatively recent result, which improved dramatically on pre-existing estimates, so improving on this, as we have done, is quite surprising. From table 2 below, we see from the second column that we find a value of the critical point very close to $1/\mu$. We can vary our estimate of a_c until we get agreement with $1/\mu$, and this

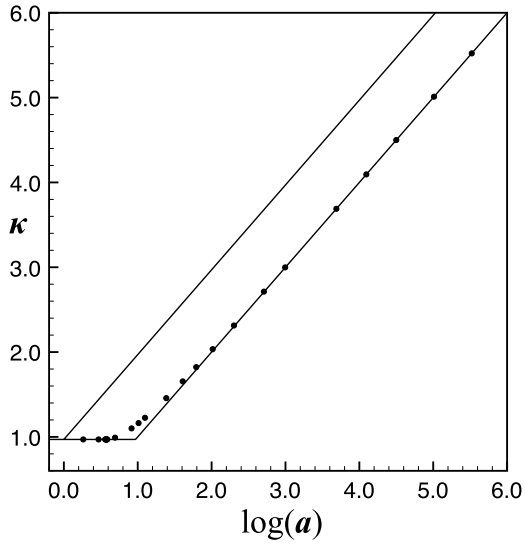

Figure 4. The a-dependence of the free energy $\kappa(a)$. The straight lines indicate the exact lower and upper bounds, where for $\log a < 0$ we know that $\kappa(a) = \log \mu$ while for $\log a > 0$ we know that $\max[\log \mu, \log a] \leqslant \kappa(a) \leqslant \log \mu + \log a$.

turns out to be at $a_c = 1.775\,615 \pm 0.000\,005$ with exponent 1.453 95 which is satisfyingly close to the conjectured exact value [2, 11] $\gamma_1^{\rm sp} = 93/64 = 1.453\,125$, where the superscript refers to the 'special' transition that takes place right at the adsorption temperature [11]. As a increases, we quickly see a simple pole emerging. So it seems that for $a = a_c$ the singularity is characterized by a (diverging) exponent $93/64$, and that this changes discontinuously to a simple pole for $a > a_c$. For $a < a_c$ the exponent is, as we would expect, given by γ_1. If we analyse the series with $y = 0$ and $a = a_c$, we can estimate the exponent γ_{11}^{sp}. We did this and found $\gamma_{11}^{sp} = 0.816 \pm 0.006$, in agreement with the expected value $13/16 = 0.8125$ [8]. In figure 4 we give our estimates of the free energy $\kappa(a) = -\log x_c$ as a function of $\log a$.

The behaviour of the anti-ferromagnetic singularity is different from that observed in the previous sub-section. For $a < a_c$ it seems stable at $-1/\mu$, with an exponent that is likely to be exactly 1.5, as for the case above. For $a > a_c$ however, the anti-ferromagnetic critical point monotonically decreases as a increases for $a > a_c$, and (conjecturally) has a square root singularity. At $a = a_c$ it looks more like a fourth root branch point, but a zero, not a divergence[4].

4.3. Phase diagram calculation

In order to locate the phase boundary between the adsorbed and ballistic phases, in the (a, y)-plane, we make use of (8). $\psi(a, y)$ is equal to $\kappa(a)$ throughout the adsorbed phase and to $\lambda(y)$ throughout the ballistic phase. The phase boundary between the adsorbed and ballistic phases is the locus of points where $\kappa(a) = \lambda(y)$. For a given value of a we calculated $\kappa(a)$ as in section 4.2 and then found the value of y such that $\lambda(y) = \kappa(a)$ by interpolating the results for $\lambda(y)$ found in section 4.1. More precisely, from table 1 we calculated $y = f_1(x_c)$ by using the program Eureqa [34] on columns 1 and 2 of table 1. As a relevant technical detail,

[4] The estimate of the singularity location is not very precise, so it is entirely possible that the exponent is not exactly $1/4$, but some fraction of approximately similar value.

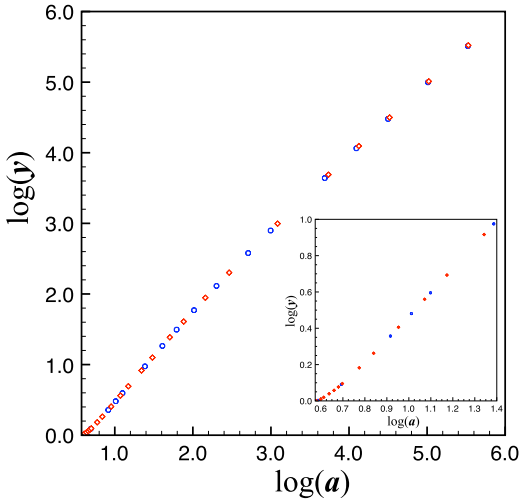

Figure 5. The phase boundary between the adsorbed and ballistic phases in the $(\log a, \log y)$-plane. The blue circles correspond to the data from table 3 while the red diamonds correspond to the data from table 4. The inset is a blow-up of the region near the origin.

Table 3. Phase diagram estimated by calculating $y(x_c)$ from the interpolation formula found by Eureqa.

a	x_c	$y(x_c)$
1.775 615	0.379 052 27	1
1.775 69	0.379 051 97	1.0001
1.8	0.378 93	1.0030
2.0	0.371 12	1.0953
2.5	0.332 682	1.4293
2.75	0.312 5387	1.6174
3.0	0.293 630 848	1.8137
4.0	0.232 915 216 03	2.6510
5.0	0.191 211 527 26	3.5399
6.0	0.161 589 812 68	4.4592
7.5	0.130 751 327 30	5.8729
10.0	0.098 924 010 46	8.2816
15.0	0.066 353 637 16	13.189
20.0	0.049 869 446 45	18.146
40	0.024 984 005 08	38.118
60	0.016 661 962 55	58.136
90	0.011 109 724 48	88.145
150	0.006 666 368 42	148.00
250	0.003 999 935 75	247.18

in actual implementation it is desirable to minimize the variation of the parameters as much as possible. Accordingly, we sought a fit to the functional form $1/y = \tilde{f}(x_c(1) - x)$ where $x_c(1) = 1/\mu = 0.379\,052\,2777\ldots$. In this way we found an interpolation formula, which we used by inserting the x_c values from table 2, so as to obtain the y values corresponding to the a values in table 2. In this way we obtained the results shown in table 3.

As a check, we also calculated points on the curve starting with a given value of y and reversing the procedure. More precisely, from table 2 we calculated $1/a = f_2(x_c)$ also by

Table 4. Phase diagram estimated by calculating $a(x_c)$ from the interpolation formula found by Eureqa.

y	x_c	$a(x_c)$
1.0	0.379 052 25	1.775 615
1.001	0.379 019	1.7854
1.01	0.378 62	1.8220
1.02	0.378 04	1.8456
1.04	0.376 49	1.8915
1.06	0.374 63	1.9347
1.08	0.372 65	1.9733
1.1	0.370 564	2.0092
1.2	0.359 2886	2.1693
1.3	0.347 5682	2.3161
1.5	0.324 9328	2.5934
1.75	0.299 554 7603	2.9206
2.0	0.277 548 710	3.2329
2.5	0.241 886 2105	3.8287
3	0.214 449 855	4.4003
4	0.175 107 0033	5.5029
5	0.148 208 714 38	6.5747
7	0.113 657 316 50	8.6708
10	0.084 421 281 92	11.757
20	0.045 635 244 07	21.876
40	0.023 835 934 09	41.923
60	0.016 661 962 55	61.912
90	0.011 109 724 48	91.864
150	0.006 666 368 42	151.74
250	0.003 999 935 75	251.50

using Eureqa on columns 1 and 2 of table 2, and found an interpolation formula. We obtained a further set of (a, y) values by substituting the x_c values from table 1, so as to obtain the a values corresponding to the y values in table 1. In this way we obtained the results shown in table 4.

Combining the data in these two tables results in the phase boundary shown in figure 5 where we have plotted the data from table 3 as red circles and the data from table 4 as blue diamonds. The close agreement between the two independent analyses implies that the results are accurate to at least graphical accuracy. The curve passes through the point (a_c^o, y_c^o), is strictly monotone increasing and asymptotic to $y = a$, as shown in [25]. It is interesting to note that the curve is not concave.

We can switch to physical variables (force and temperature) using (2). Without much loss of generality we can set $\epsilon = -1$ and work in units where $k_B = 1$. The corresponding phase boundary in the force–temperature plane is given in figure 6. Notice that the force at zero T is 1 and the limiting slope at $T = 0$ is zero, as predicted in [25]. The curve is monotone decreasing as T increases, with no re-entrance. See for instance [25, 30, 36] for further discussion. The force–temperature curve is in semi-quantitative agreement with an earlier numerical study by Mishra *et al* [30], but is substantially more precise.

5. The behaviour and nature of the phase transition on the phase boundary

It is possible to use the results of [25] to prove that the phase transition from the ballistic to the adsorbed phase is first order. We state this as a theorem.

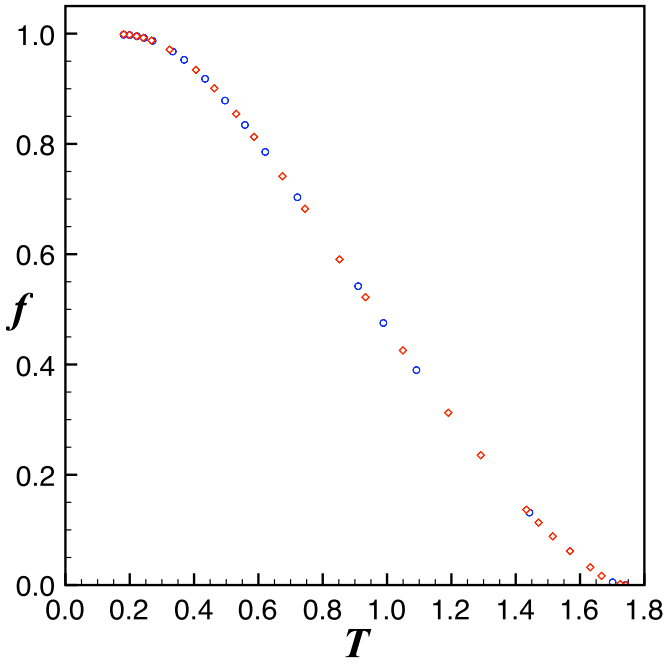

Figure 6. The phase boundary given as a force–temperature diagram. The horizontal axis is $T = \frac{1}{\log(a)}$, the vertical axis is the force, $f = \frac{\log(y)}{\log(a)}$.

Theorem 1. *The free energy $\psi(a, y)$ is not differentiable at the phase boundary between the ballistic and adsorbed phases, except perhaps at the point (a_c^o, y_c^o).*

Proof. There is a monotone strictly increasing curve $y = y_c(a)$ in the (a, y)-plane, through the point (a_c^o, y_c^o), corresponding to the phase boundary between the ballistic and adsorbed phases. In the ballistic phase $\psi(a, y) = \lambda(y)$ and in the adsorbed phase $\psi(a, y) = \kappa(a)$. The free energy $\kappa(a)$ is a monotone increasing function of a, convex in $\log a$. It therefore has left and right derivatives at every value of a. Throughout the adsorbed phase the left and right derivatives of $\kappa(a)$ are positive. Consider a line of fixed $y = y_1 > y_c^0 \geqslant 1$. The free energy $\psi(a, y_1) = \lambda(y_1)$ for $a \leqslant a_c(y_1)$ and $\psi(a, y_1) = \kappa(a)$ for $a \geqslant a_c(y_1)$. For $a \leqslant a_c(y_1)$, $\partial\psi(a, y_1)/\partial a = 0$. For $a \geqslant a_c(y_1)$ the right derivative of $\kappa(a)$ with respect to a is positive. Therefore the left and right derivatives of $\psi(a, y)$ with respect to a at $(a_c(y_1), y_1)$ are not equal and the free energy is not differentiable. □

However it is still of interest to determine how the free energy behaves as we approach the phase boundary. We 'know' the location of the phase boundary from the results reported in the previous section, at least to graphical accuracy. That is to say, with an accuracy of three to four significant digits. At the phase boundary, we also know the value of the radius of convergence, from the data above. So, by way of example, at $a = 2$ the phase boundary is at $y = 1.095$. If we analyse the series at this point, (recall this just means substituting the required values of a and y into the three-variable generating function we have, which produces a one-variable generating function, where the expansion variable is conjugate to the length of the walk) we find the critical point is at $x_c = 0.371\,125$ with an exponent of -1.995. This is exactly the same value of x_c found at $a = 2,\ y = 1$, though at $(2, 1)$ the exponent is a simple pole.

As we increase y, we see exactly the same behaviour as observed in section 1 that allowed us to identify a_c. That is to say, there is a variation in the critical point and critical exponent as the approximants struggle to cope with a discontinuous exponent change. So at $(2, 1.05)$ the $(x_c, \textit{exponent})$ pair is estimated to be $(0.371\,35, -1.36 \pm 0.3)$. This large error in the exponent estimate is a signature that the analysis method is struggling. At $(2, 1.09)$ we find $(0.371\,325, -1.962 \pm 0.016)$, and at $(2, 1.095)$, which is our best estimate of the intersection of the line $a = 2$ with the phase boundary, we find for the critical point and exponent $(0.371\,125, -1.998 \pm 0.013)$. Note that this value of the critical point is exactly that found when $a = 2$ and $y = 1$, which is well below the phase boundary.

Suggestive as this is, we note that the value of a chosen is rather close to the point (a_c, y_c) (a bicritical point, see [28]), where the behaviour is different, and may still have an effect on the convergence rate of the series. So we take another example, when $a = 3$, which is well away from the point (a_c, y_c). At $(3, 1)$ the critical point is $x_c = 0.293\,6308\ldots$, and the exponent is a simple pole. The phase boundary point at $a = 3$ is estimated to be at $y = 1.8137$. Analysis of the series at that point gives $(0.293\,636, -2.0001 \pm 0.0002)$, rather confirming the double pole. The location is slightly different from that observed at $(a = 3, y = 1)$, but that is likely ascribable to the estimate of y on the phase boundary being slightly in error. Indeed, if we repeat the analysis with $y = 1.8139$, we find $x_c = 0.293\,627\ldots$, and the exponent estimate is $-2.000\,0018 \pm 0.000\,0022$, which is rather convincing evidence for a double pole!

So we find that at (or very near to and below) the phase boundary, the series are well-converged, give the estimates of the critical point we expect, and display a double pole singularity. Near to the phase boundary, the estimates are very variable, and behave in exactly the same way as did the series analysed in section 4, with the approximants seemingly struggling to cope with a discontinuous change in the critical exponent.

It is instructive to consider the simpler case of directed positive walks. We discuss two cases:

(1) positive walks with step set $(1, 1)$ and $(1, -1)$, which we refer to loosely as Dyck paths, and
(2) positive walks with step set $(1, 1)$, $(1, -1)$ and $(1, 0)$, which we refer to loosely as Motzkin paths.

It is straightforward to solve each of these models exactly, though we do not give the details here. They each show three phases (a free phase, an adsorbed phase and a ballistic phase). There is a phase boundary between the adsorbed and ballistic phases and in both cases these phase boundaries are concave in the $(\log a, \log y)$-plane. In the Motzkin path case the phase boundary is asymptotic to $y = a$ while in the Dyck path case it is asymptotic to $y = a^{1/2}$, because a maximum of half the vertices can be in the surface. In each case the singularity in both the adsorbed and ballistic phases is a simple pole so the generating function has both of these singularities though one is dominant in the adsorbed phase and the other is dominant in the ballistic phase. On the phase boundary between the adsorbed and ballistic phases these two singularities are equal resulting in a double pole, just as observed numerically for the case of SAWs.

6. Discussion

We have considered a SAW model of polymer adsorption at an impenetrable surface where

(1) the walk is terminally attached to the surface,
(2) the walk interacts with the surface with an attractive potential, and
(3) the walk is subject to a force applied normal to the surface at the last vertex of the walk.

For the square lattice we have used series analysis techniques to investigate the phases and phase boundaries for the system. There are three phases, a free phase where the walk is desorbed but not ballistic, an adsorbed phase where the walk is adsorbed at the surface and a ballistic phase where the walk is desorbed but ballistic. We have located the phase boundaries and proved that the phase transition from the adsorbed to the ballistic phase is first order. In addition we have very precise values for the critical points for adsorption without a force and for the free to ballistic transition with no surface interaction.

Acknowledgments

The authors would like to acknowledge helpful conversations with Enzo Orlandini, and help with the preparation of the data files by Jason Whyte. This research was partially supported by NSERC of Canada. The computations for this work were supported by an award to IJ under the Merit Allocation Scheme on the NCI National Facility at the Australian National University. IJ and AJG were supported under the Australian Research Council's Discovery Projects funding scheme by the grants DP120101593 and DP120100939 respectively. We thank Cornell Creative Machines Lab for making available the program Eurequa [34].

References

[1] Barber M N, Guttmann A J, Middlemiss K M, Torrie G M and Whittington S G 1978 *J. Phys. A: Math. Gen.* **11** 1833–42
[2] Batchelor M T and Yung C M 1995 *Phys. Rev. Lett.* **74** 2026–9
[3] Beaton N R, Guttmann A J and Jensen I 2012 *J. Phys. A: Math. Theor.* **45** 055208
[4] Cardy J L 1984 *Nucl. Phys.* B **240** 514–32
[5] Clisby N and Jensen I 2012 *J. Phys. A: Math. Theor.* **45** 115202
[6] Conway A R, Enting I G and Guttmann A J 1993 *J. Phys. A: Math. Gen.* **26** 1519–34
[7] De'Bell K and Lookman T 1993 *Rev. Mod. Phys.* **65** 87–113
[8] Duplantier B and Saleur H 1986 *Phys. Rev. Lett.* **57** 3179–82
[9] Enting I G 1980 *J. Phys. A: Math. Gen.* **13** 3713–22
[10] Forgacs G, Privman V and Frisch H L 1989 *J. Chem. Phys.* **90** 3339–45
[11] Guim I and Burkhardt T W 1989 *J. Phys. A: Math. Gen.* **22** 1131–40
[12] Guttmann A J and Jensen I 2009 *Polygons, Polyominoes and Polycubes (Lecture Notes in Physics* vol 775*)* ed A J Guttmann (Berlin: Springer)
[13] Hammersley J M 1982 *J. Appl. Probab.* **19** 327–31
[14] Hammersley J M and Morton K W 1954 *J. R. Stat. Soc.* B **16** 23–38
[15] Hammersley J M, Torrie G M and Whittington S G 1982 *J. Phys. A: Math. Gen.* **15** 539–71
[16] Haupt B J, Ennis J and Sevick E M 1999 *Langmuir* **15** 3886–389
[17] Hegger R and Grassberger P 1994 *J. Phys. A: Math. Gen.* **27** 4069–81
[18] Iliev G K, Orlandini E and Whittington S G 2013 *J. Phys. A: Math. Theor.* **46** 055001
[19] Ioffe D and Velenik Y 2008 Ballistic phase of self-interacting random walks *Analysis and Stochastics of Growth Processes and Interface Models* ed P Morters, R Moser, M Penrose, H Schwetlick and J Zimmer (Oxford: Oxford University Press) pp 55–79
[20] Janse van Rensburg E J 1998 *J. Phys. A: Math. Gen.* **31** 8295–306
[21] Janse van Rensburg E J 2000 *The Statistical Mechanics of Interacting Walks, Polygons, Animals and Vesicles* (Oxford: Oxford University Press)
[22] Janse van Rensburg E J 2003 *J. Phys. A: Math. Gen.* **36** R11–61
[23] Janse van Rensburg E J, Orlandini E, Tesi M C and Whittington S G 2009 *J. Stat. Mech.* **2009** P07014
[24] Janse van Rensburg E J and Rechnitzer A 2004 *J. Phys. A: Math. Gen.* **37** 6875–98
[25] Janse van Rensburg E J and Whittington S G 2013 *J. Phys. A: Math. Theor.* **46** 435003
[26] Jensen I 2004 *J. Phys. A: Math. Gen.* **37** 5503–24
[27] Jensen I 2013 A new transfer-matrix algorithm for exact enumerations: self-avoiding walks on the square lattice arXiv:1309.6709

[28] Klushin L I, Skvortsov A M and Gorbunov A A 1997 *Phys. Rev.* E **56** 1511–21
[29] Krawczyk J, Owczarek A L, Prellberg T and Rechnitzer A 2005 *J. Stat. Mech.* **2005** P05008
[30] Mishra P K, Kumar S and Singh Y 2005 *Europhys. Lett.* **69** 102–8
[31] Orlandini E, Tesi M C and Whittington S G 1999 *J. Phys. A: Math. Gen.* **32** 469–77
[32] Owczarek A L 2010 *J. Phys. A: Math. Theor.* **43** 225002
[33] Rubin R J 1965 *J. Chem. Phys.* **43** 2392–407
[34] Schmidt M and Lipson H 2009 *Science* **324** 81–85
[35] Silberberg A 1962 *J. Phys. Chem.* **66** 1872–83
[36] Skvortsov A M, Klushin L I, Fleer G J and Leermakers F A M 2009 *J. Chem. Phys.* **130** 174704
[37] Skvortsov A M, Klushin L I, Polotsky A A and Binder K 2012 *Phys. Rev.* E **85** 031803
[38] Whittington S G 1975 *J. Chem. Phys.* **63** 779–85
[39] Whittington S G 1998 *J. Phys. A: Math. Gen.* **31** 8797–803
[40] Zhang W and Zhang X 2003 *Prog. Polym. Sci.* **28** 1271–95